Nathans, D., Notani, G., Schwarz, J. H., & Zinder, N. D. (1962) *Proc. Natl. Acad. Sci. U.S.A. 48*, 1424–1431.
Nathans, D., Oeschger, M., Polmar, S. K., & Eggen, K. (1969) *J. Mol. Biol. 39*, 279–292.
Nomura, M., Tissieres, A., & Lengyel, P. (1974) *Ribosomes*, Cold Spring Harbor Laboratory, Cold Spring Harbor, NY.
Pestka, S. (1969) *J. Biol. Chem. 244*, 1533–1539.
Pestka, S. (1970) *Arch. Biochem. Biophys. 136*, 80–88.
Pestka, S. (1972) *Proc. Natl. Acad. Sci. U.S.A. 69*, 624–628.
Revel, M., Pollack, Y., Groner, Y., Scheps, R., Inouye, H., Berissi, H., & Zeller, H. (1973) *Biochimie 55*, 41–51.
Saltzman, L. A., Brown, M., & Apirion, D. (1974) *Mol. Gen. Genet. 133*, 201–207.
Schaup, H. W., Green, M., & Kurland, C. G. (1970) *Mol. Gen. Genet. 109*, 193–205.
Schlessinger, D. (1974) *Annu. Rev. Genet. 8*, 135–154.
Spirin, A. S. (1978) *Prog. Nucleic Acid Res. Mol. Biol. 21*, 39–62.
Stöffler, G., & Wittmann, H. G. (1977) in *Molecular Mechanisms of Protein Biosynthesis* (Weissbach, H., & Pestka, S., Eds.) pp 117–202, Academic Press, New York.
Strauss, J. H., & Sinsheimer, R. L. (1963) *J. Mol. Biol. 7*, 43–54.
Sugiyama, T., & Nakada, D. (1968) *J. Mol. Biol. 31*, 431–440.
Tai, P.-C., Wallace, B. J., Herzog, E. L., & Davis, B. D. (1973) *Biochemistry 12*, 609–615.
Traub, P., & Nomura, M. (1969) *J. Mol. Biol. 40*, 391–413.
Traub, P., Mizushima, S., Lowry, C. V., & Nomura, M. (1971) *Methods Enzymol. 20*, 391–407.
Weber, K., & Osborn, M. (1969) *J. Biol. Chem. 244*, 4406–4412.
Weissbach, H., & Pestka, S. (1977) *Molecular Mechanisms of Protein Biosynthesis*, Academic Press, New York.
Zamir, A., Miskin, R., Vogel, Z., & Elson, D. (1974) *Methods Enzymol. 30*, 406–426.

Direct Iodination of Specific Residues in Crystals of Yeast Formylatable Methionine-Accepting Transfer Ribonucleic Acid†

James Tropp‡ and Paul B. Sigler*

ABSTRACT: Crystals of yeast formylatable methionine-accepting transfer ribonucleic acid (tRNA$_f^{Met}$) were iodinated by using a modification of Commerford's procedure [Commerford, S. L. (1971) *Biochemistry 10*, 1993]. Chromatographic analysis of nuclease digestion products showed that radioactive iodine binds covalently to the 5 position of three nucleotide residues: U_8, C_{73}, and C_{74}. These three iodine substitutions were assigned to three peaks in a difference Fourier synthesis comparing the iodinated derivative with native tRNA$_f^{Met}$. In this way the positions of U_8, C_{73}, and C_{74} were marked in the crystal structure of yeast tRNA$_f^{Met}$, providing guidepoints for the interpretation of a 4.5-Å electron density map.

The interpretation of electron density maps from X-ray diffraction studies of macromolecules is facilitated by isomorphous derivatives which mark specific residues with heavy atoms. One can combine X-ray diffraction and chemical sequencing methods to map the heavy-atom binding sites in the crystal onto their corresponding locations in the sequence, thus providing guidepoints for tracing the molecular backbone (Sigler et al., 1966; Dunill et al., 1966; Pasek et al., 1973; Rosa & Sigler, 1974; Schevitz et al., 1975). In certain cases, the markers can be used to establish the relative orientation and position of similar structures in different crystal forms (Matthews et al., 1968; Wyckoff et al., 1969; Sigler, 1970).

The heavy atom employed as a marker should satisfy the following criteria. (a) It should have an atomic number high enough to be readily located in a difference Fourier synthesis. (b) It should react covalently under mild conditions. (c) Its binding should not distort the crystal structure. (d) It should possess convenient radioisotopes to facilitate finding its position in the sequence. Iodine is a natural choice.

Commerford (1971) has shown that a mixture of KI and $TlCl_3$ will iodinate polynucleotides in solution with a strong preference for single-stranded pyrimidine residues. The reaction proceeds in two steps (Figure 1): first, a rapid uptake of iodine to form a labile intermediate, followed by conversion to products or reversion to starting materials (Commerford, 1971; Anderson & Folk, 1976). Both poly(C) and poly(U) incorporate comparable amounts of iodine in the first step, but conversion to iodopyrimidine is much greater for poly(C) (Commerford, 1971). Schmidt et al. (1973) iodinated yeast tRNA$_f^{Met}$ in solution by this method and presented evidence for the iodination of three cytidines, two at the 3′-terminal C-C-A end and one in the anticodon loop. Recently, Batey & Brown (1977) iodinated several tRNA species and found that they could iodinate only C residues which were considered "exposed" by other criteria. We have employed a modification of Commerford's method to iodinate crystals of yeast tRNA$_f^{Met}$ directly. To facilitate the chemical analysis, we have used ^{125}I in all experiments. We have shown that there are three major sites to which iodine is covalently attached, namely, the 5 position of residues U_8, C_{73}, and C_{74}, and have assigned these covalently bound iodine atoms to three peaks in a difference

† From the Department of Biochemistry and the Department of Biophysics and Theoretical Biology, The University of Chicago, Chicago, Illinois 60637. *Received September 25, 1978; revised manuscript received September 12, 1979.* Supported by National Science Foundation Grant GB97654 (PCM74 15075) and by the National Institutes of Health, U.S. Public Health Service, Grant GM 15225. J.T. was partially supported by U.S. Public Health Service Training Grant PHS GM-424.
‡ Present address: Department of Chemistry, Brandeis University, Waltham, MA 02154.

0006-2960/79/0418-5489$01.00/0

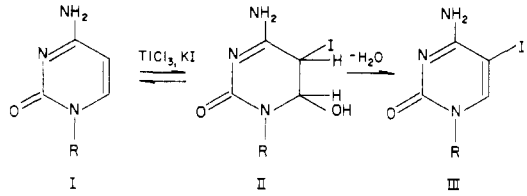

FIGURE 1: Iodination of pyrimidines, here shown for cytidine. The structure of intermediate II is hypothetical.

Fourier synthesis comparing the iodo derivative[1] to the native $tRNA_f^{Met}$. These three heavy-atom markers proved to be quite helpful in the interpretation of the 4.5-Å electron density map of crystalline yeast $tRNA_f^{Met}$ (Schevitz et al., 1979).

Materials and Methods

Reagents. Thallium trichloride (Alfa Inorganics) was used without purification; 0.10 M solutions were prepared immediately prior to use. Potassium iodide was reagent grade; radioactive solutions were prepared by adding small volumes (10–50 μL) of carrier-free [^{125}I]NaI (Amersham, New England Nuclear) to 10 mL of a 5 mM KI stock solution. These solutions were stable for months in the dark at room temperature. All nucleosides were purchased from Sigma Chemicals and used without purification. All other chemicals were reagent grade.

Crystals of Yeast $tRNA_f^{Met}$. $tRNA_f^{Met}$ from baker's yeast was purified, and crystals were grown as described previously (Johnson et al., 1970; Pasek et al., 1973). Prior to iodination the crystals were stabilized in a tRNA-free supernatant solution containing 2.9 M $(NH_4)_2SO_4$, 5 mM $MgCl_2$, 5 mM sodium cacodylate, and 2 mM spermine, pH 5.9 (Johnson et al., 1970).

Measurement of Radioactivity. ^{125}I radioactivity was determined in a Nuclear Chicago well-type γ counter (detector Model DS 207(V), analyzer Model 8725). Samples were counted either in test tubes or in Nuclear Chicago well vials. Standard solutions showed that the counting efficiency was ~30% in both cases.

Preparation of the Iodo Derivative. Several crystals (10–15 nmol of yeast $tRNA_f^{Met}$) were washed in a modified stabilizing solution containing 2.9 M $(NH_4)_2SO_4$, 5 mM $MgCl_2$, and 5 mM sodium cacodylate, pH 5.0. Crystals were then flame-sealed in an ampule containing 2 mL of freshly prepared iodinating soak solution [2.9 M $(NH_4)_2SO_4$, 5 mM $MgCl_2$, 5 mM sodium cacodylate, 0.12 mM [^{125}I]KI, and 0.75 mM $TlCl_3$, pH 5.0]. After being incubated in the dark at room temperature for 96 h, the crystals were rinsed clean of unreacted KI and $TlCl_3$ by repeated cycles of washing and equilibrating with fresh modified stabilizing solution, typically eight or nine cycles over 2 days. Attempts to reequilibrate iodinated crystals with normal stabilizing supernatant caused severe cracking and yellowing of the crystals.

Control reactions to test for (a) iodination in the absence of $TlCl_3$, (b) binding of Tl^{3+}, and (c) binding of Tl^{1+} were performed as above with the following modifications of the soak solutions: (a) $TlCl_3$ omitted; (b) KI omitted; (c) KI omitted and TlCl substituted for $TlCl_3$.

Enzyme Stock Solutions. RNase T_1 (Calbiochem) solution was 5000 units/mL in 0.01 M Tris-HCl, pH 7.5, and was heat-treated to inactivate phosphatase contaminants (Reeves et al., 1968). Snake venom phosphodiesterase (Worthington) was 0.8 mg/mL by absorbance at 278 nm in a 1:1 (v/v) mixture of glycerol and 0.01 M Tris-HCl, 0.01 M $MgCl_2$, pH 8.7. Pancreatic RNase (Sigma) was 1 mg/mL in 0.10 M Tris-HCl and 0.01 M $MgCl_2$, pH 8.0. A mixed nuclease–phosphatase solution contained 1 mg each of pancreatic RNase, snake venom phosphodiesterase, and bacterial alkaline phosphatase (Worthington BAPF) in 1 mL of 0.10 M Tris-HCl and 0.01 M $MgCl_2$, pH 8.0.

Enzyme Digests and Chromatographic Analysis. The sequence positions of iodinated residues were identified by analysis of RNase T_1 cleavage fragments from the iodo derivative. RNase T_1 digestion was performed as described by Rosa & Sigler (1974), and cleavage fragments were separated by high-pressure column chromatography on Al-Pellionex-WAX (Whatman) (Rosa & Sigler, 1974) and Vydac-SAX (Separations Group). The iodinated fragments were characterized by further digestion with pancreatic RNase or the nuclease–phosphatase mixture (Rosa & Sigler, 1974). The nucleoside products of these digests were identified and quantitated by chromatography on Aminex A-6 (Bio-Rad) (Uziel et al., 1968; Rosa & Sigler, 1974). All column effluents were continuously monitored at 254 nm with an Altex 154 UV analyzer; radioiodinated fragments were located in the effluents by counting fractions directly.

Nucleoside analyses were performed on Aminex A-6, following Rosa & Sigler (1974). Nucleosides were identified by the time interval (constant flow) between sample injection and appearance of the peak in the elution profile. These elution times were established by calibration with authentic standards and were highly reproducible. An adequate separation of nucleosides was achieved in all cases (Figure 2). The common nucleosides, adenosine, guanosine, uridine, and cytidine, were easily quantitated since their peak heights in the elution profile at 254 nm are linearly proportional to the amount of nucleoside applied to the column. It was difficult to quantitate the modified nucleosides 1-methylguanosine and N^2-methylguanosine because of irreproducible standards, and values for these nucleosides were not considered reliable beyond a factor of 2. The iodinated nucleosides 5-iodocytidine and 5-iodouridine were quantitated by counting ^{125}I since these nucleosides absorb weakly at 254 nm and elute too close to adenosine and 1-methylguanosine, respectively, to give resolved peaks when large amounts of the latter two are present (Figure 2).

X-ray Crystallography. Ninety percent of the intensities to 6-Å resolution were obtained from precession photographs of the iodo derivative taken with Cu Kα radiation from an Elliott GX6 generator fitted with a graphite monochromator (Navia, 1974). The corresponding data for the parent structure, collected in a similar way, were given to us by Dr. R. W. Schevitz. Crystal temperature was maintained at 3 °C with a stream of cold dry air from a device similar to that of Marsh & Petsko (1973), except that the cooling bath was replaced by a heat exchanger consisting of a fin tube cooled by the cold probe of a Neslab Cryocool unit (Tropp, 1976). Derivative crystals were much more radiation sensitive than were native crystals. Crystal decay in the X-ray beam was apparently both time and dose dependent.

The intensities of both the parent and iodo derivative were retrieved from the photos in digital form by an Optronics P-100 densitometer interfaced to a PDP 11/40, employing the SCA-N11 densitometry package (P. H. Bethge, unpublished experiments). Lorentz–polarization-corrected and symmetry-averaged structure amplitudes of the derivative were scaled

[1] Iodo derivative refers to the irreversibly iodinated crystalline yeast $tRNA_f^{Met}$ molecule. $tRNA_f^{Met}$ is the species of methionine-accepting tRNA which initiates protein synthesis and is identified here by the capacity of its methionine adduct to be formylated by the *Escherichia coli* transformylase (RajBhandary & Ghosh, 1969).

Table I: Stoichiometry of Iodine Incorporation

sample	iodinating reagents[a]	purifn	cpm[b]	A_{258} unit	g-atoms of iodine per mole of tRNA[c,d]
1	KI and $TlCl_3$	DEAE[e]	2.11×10^4	0.27	2.10
2	KI and $TlCl_3$	DEAE[f]	1.27×10^4	0.18	1.90[i]
3	KI and $TlCl_3$	gel filtration[g]	1.65×10^4	0.23	1.93
4	KI	none[h]	0.0	0.21	0.0

[a] Crystals were reacted and washed free of iodinating reagents as described under Materials and Methods. [b] Background subtracted. [c] Based on a molecular weight of 24 600 (Simsek & RajBhandary, 1972) and 20 A_{258} units/mg of yeast tRNA$_f^{Met}$. [d] Specific activity of ^{125}I was 1.86×10^4 cpm/nmol. [e] Stabilizing supernatant was removed, crystals were dissolved in 1 mL of buffer A (0.10 M NaCl, 5 mM $MgCl_2$, and 0.10 M Tris-HCl, pH 7.5), applied to DEAE-cellulose, and washed with buffer A until no radioactivity eluted, and then tRNA was eluted with buffer B (same as buffer A, except 1.2 M NaCl). Ninety percent of the total radioactivity applied to DEAE-cellulose was recovered; 10% of the recovered radioactivity was in the buffer A wash. [f] As in footnote *e* but tRNA was first heated to 50 °C in 0.1 M NaCl, 5 mM EDTA, and 0.10 M sodium acetate, pH 4.0, for 1 min and applied to the column equilibrated with the same buffer. The column was washed with same low pH buffer and then with buffer A and then eluted with buffer B. The eluate was then heated to 50 °C for 1 min and allowed to cool. [g] tRNA was dissolved in buffer A and then passed over G-25 equilibrated with buffer A. [h] Crystals were completely free of radioactivity after being washed as in footnote *a*, and no further purification was required. [i] Assumes that tRNA was completely renatured.

plane by plane to the parent amplitudes, and a three-dimensional difference Fourier synthesis was calculated as described in the legend to Figure 10. Occupancies and positional parameters for heavy-atom sites identified on the difference synthesis were refined by using a modification (R. W. Schevitz, unpublished experiments) of the program REFINE (Adams et al., 1969).

Results

Stoichiometry of Iodination. Table I shows the stoichiometry of iodine incorporation. Crystals began to crack severely as the level of iodination reached 3 g-atoms of iodine per mol of tRNA$_f^{Met}$.

A small fraction (~10%) of the iodine covalently bound to crystalline tRNA$_f^{Met}$ appeared to bind in a labile form. This was concluded from the following observations. (a) Crystals soaked with $TlCl_3$ and KI exhibited a small persistent leaching of radioactivity (10^{-6} M) into the stabilizing supernatant, whereas this was not seen in crystals soaked with radioactive KI alone. This indicates that the radioactivity did not come from residual iodide ion entrained in the interstices. (b) When the crystalline iodo derivative was dissolved and applied to DEAE-cellulose, 10% of the radioactivity was recovered in the buffer A wash (Table I), which was at least 100 times more than one can account for by "thermal" exchange assuming that the iodide concentration in the crystal's interstices was not significantly greater than the iodide concentration in the supernatant solution. In any case, the labile iodine components did not confound the chemical analysis of the covalent binding sites since all samples of the iodo derivative were subjected to chromatography on DEAE or gel filtration prior to further chemical analysis.

Iodine Is Covalently Bound as 5-Iodocytidine and 5-Iodouridine. Figure 2 shows the Aminex A-6 elution profile for the mixed nuclease–phosphatase digest of the iodo derivative. Iodine was covalently bound as 5-iodocytidine and 5-iodouridine in the ratio of ~2.4:1. Free iodide derived from the

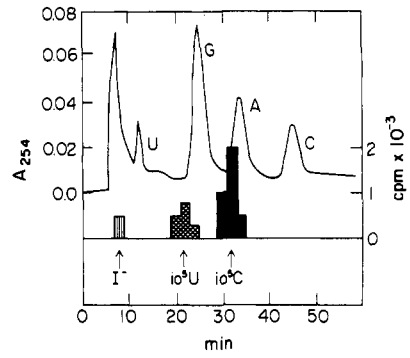

FIGURE 2: Nucleoside analysis of iodo derivative on Aminex A-6. 100 pmol of derivative was digested with the nuclease–phosphatase mixture (see Materials and Methods) and chromatographed on Aminex as described by Rosa & Sigler (1974). The large leftmost peak at the solvent front is due to elution of the enzymes. The histogram shows ^{125}I radioactivity and is coded to indicate the radioactive species: (vertical stripe) I^-, (crosshatch) 5-iodouridine; (black) 5-iodocytidine. The radioactivity was assigned to these species by virtue of the fact that authentic samples of these compounds elute at precisely the indicated positions.

breakdown of labile addition products (see above) eluted with the solvent front and comprised roughly 10% of the total recovered iodine.

Figure 3a shows the Pellionex elution profile for the RNase T_1 digest of native yeast tRNA$_f^{Met}$; the peak assignments are given in Rosa & Sigler (1974). Figure 3b shows the Pellionex profile for the RNase T_1 digest of the iodo derivative. Four peaks in the elution profile contained significant levels of covalently bound iodine. Nucleoside composition analysis on Aminex showed that two of these peaks, 9 and 11, contained iodine incorporated exclusively as 5-iodocytidine, and the other two peaks, 1 and 10, contained iodine exclusively as 5-iodouridine. The ratio of 5-iodocytidine/5-iodouridine was ~2:1, in rough agreement with the nucleoside analysis. A single nucleoside analysis did not always permit immediate and positive identification of an iodinated oligonucleotide because the radioactive oligonucleotide is often overlapped with other cleavage fragments in the elution profile. As an example, the analysis of fragment 1b is shown in Figure 4 (see the legend to Figure 3 for the alphanumerical designation of peaks in the elution profiles). The iodinated oligonucleotides were identified as described below. Refer to Figure 5 for the sequence of yeast tRNA$_f^{Met}$, where the relevant RNase T_1 cleavage fragments are delineated.

Iodination of Cytidine Occurs at C_{73} and C_{74}. Comparison of Figures 3b and 3c shows that limited digestion of the iodo derivative with snake venom phosphodiesterase prior to RNase T_1 digestion shifted the elution positions of the two peaks in Figure 3b containing 5-iodocytidine while the peaks containing 5-iodouridine were unaffected. Studies with native yeast tRNA$_f^{Met}$ (Pasek et al., 1973) have shown that sensitivity to limited phosphodiesterase digestion is unique to the 3′-terminal hexanucleotide; therefore, it is clear that all of the 5-iodocytidine of the iodo derivative is contained in the 3′-terminal hexanucleotide. No radioactivity was found at the normal elution position for C-U-A-C-C-A; thus, iodination of cytidine altered the Pellionex mobility of the 3′-terminal hexamer. This is consistent with the reduction of the pK_a of cytidine which accompanies halogenation and thereby causes increased retardation of the less protonated iodocytidine residues by the positively charged Pellionex matrix.

To confirm that 5-iodocytidine was incorporated at the 3′-terminal hexanucleotide and to establish the stoichiometry of iodination in each iodinated fragment, the elution peaks 9b

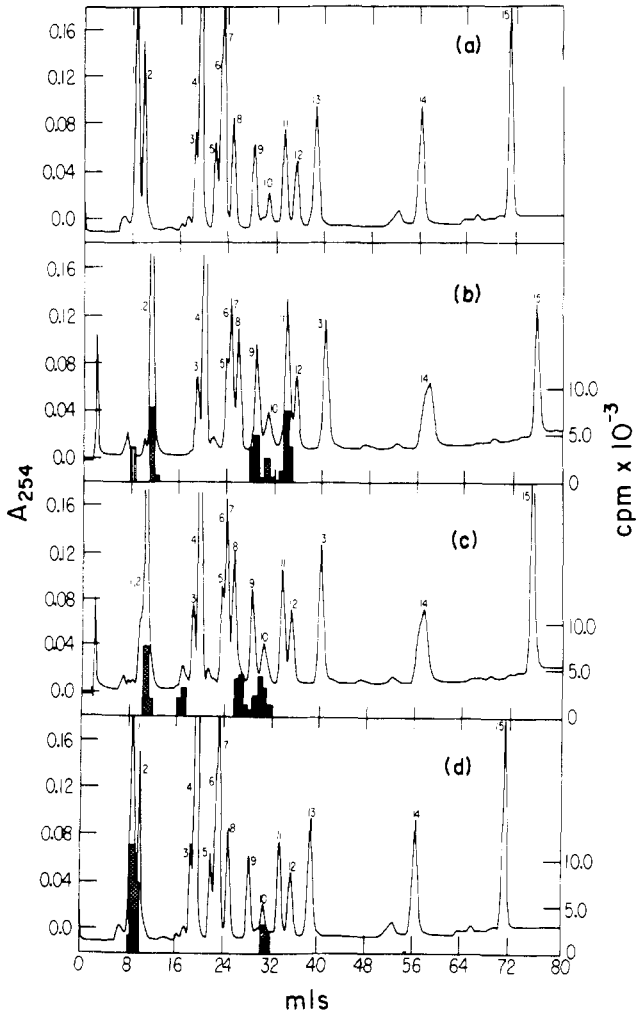

FIGURE 3: Pellionex chromatography of RNase T_1 digests of native yeast $tRNA_f^{Met}$ and its iodo derivative. (a) 2 A_{258} units of $tRNA_f^{Met}$. (b) 2 A_{258} units of iodo derivative. (c) 2 A_{258} units of iodo derivative following limited treatment with snake venom phosphodiesterase. 2 A_{258} units was digested with venom phosphodiesterase following Pasek et al. (1973), and the reaction mixture was then applied to DEAE-cellulose, washed with water, and eluted with 2 M triethylammonium bicarbonate, pH 9. The elutant was lyophilized and digested with RNase T_1 as described. (d) Further RNase T_1 digest of elution peak 10b (Figure 3b). Appropriate fractions were collected and lyophilized as described in Figure 4. The resulting powder was then dissolved in 25 μL of 0.01 M Tris-HCl, pH 7.5, and incubated with 5 units of RNase T_1 for 1 h at 37 °C. The reaction mixture was then pooled with 2 A_{258} units of previously T_1-digested native $tRNA_f^{Met}$ to serve as carrier and calibration. Pellionex chromatography was performed following Rosa & Sigler (1974) in all cases above. The solid line is A_{254}. The histograms are ^{125}I radioactivity and are coded to indicate the radioactive species as determined by nucleoside analysis of radioactive peaks: (black) 5-iodocytidine; (crosshatched) 5-iodouridine; (vertical stripe) I^-. Elution peaks are referred to in the text by a number and a letter script; the numbers correspond to the peak labels on the figure, and the scripts a, b, c, and d specify which of the four profiles in Figure 3 is being referred to.

and 11b (Figure 3b) were digested with pancreatic RNase and chromatographed on Aminex A-6 (Figure 6). Note that Aminex chromatography excludes nucleotides but separates and quantitates nucleosides. Pancreatic RNase digestion of either intact $tRNA_f^{Met}$ or its RNase T_1 digestion products releases free adenosine only from the molecular 3′ terminus. Thus, the amount of adenosine found in an Aminex analysis of a digest of elution peaks 9b and 11b (Figure 6) is a direct measure of the amount of 3′-terminal hexanucleotide which was present in those fractions, regardless of the overlapping T_1 fragments. Furthermore, pancreatic RNase releases 5-

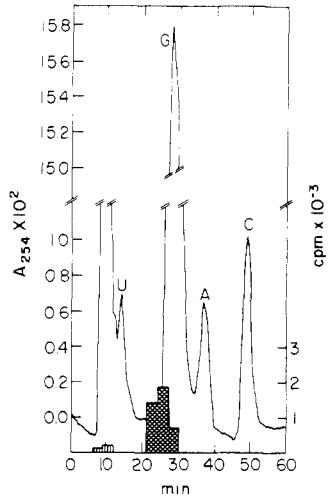

FIGURE 4: Apparent nucleoside composition of a radioactive RNase T_1 cleavage fragment (fragment 1b) overlapped with other digestion products. Appropriate fractions from Pellionex were pooled, diluted with H_2O, applied to a 0.3-mL DEAE-cellulose column, washed with water, and eluted with 2 M triethylammonium bicarbonate, pH 9.0. The eluate was lyophilized and digested with the nuclease–phosphatase mixture (see Materials and Methods). Aminex chromatography was performed as noted in the legend to Figure 2. The histogram indicates the radioactivity due to [^{125}I]-5-iodouridine. The leftmost peak is due to enzyme and is off scale. The radioactive fragment was shown to be io^5Upm^1Gp.

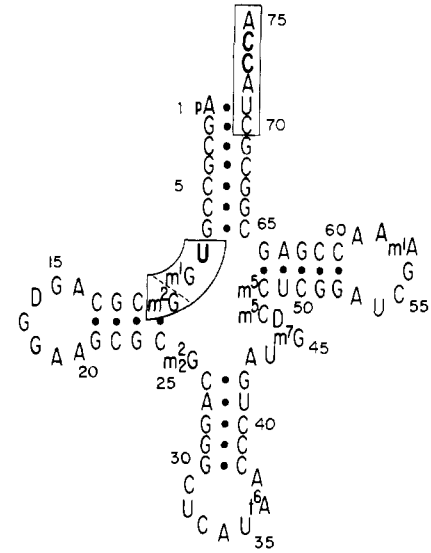

FIGURE 5: Sequence of yeast $tRNA_f^{Met}$ (Simsek & RajBhandary, 1972) with radioactive RNase T_1 cleavage fragments enclosed in boxes. The dashed line indicates a point where RNase T_1 cleavage is not complete under the digestion conditions used here. Reactive residues are slightly accentuated.

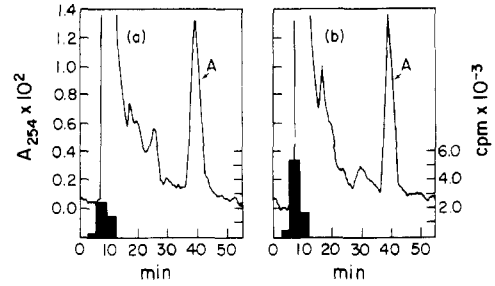

FIGURE 6: Aminex A-6 chromatography of pancreatic RNase digests of RNase T_1 elution peaks containing the 3′-terminal hexanucleotide of the iodo derivative. (a) Digest of peak 9b. (b) Digest of peak 11b. Details of the digest and chromatography are given under Materials and Methods and the legend to Figure 4.

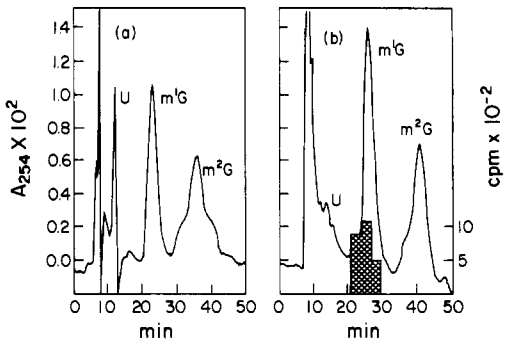

FIGURE 7: Nucleoside composition analysis of Aminex A-6 chromatography of (a) peak 10a of Figure 3a (native) and (b) peak 10b of Figure 3b (iodo derivative). Experimental details were the same as those given in Figure 4. The histogram indicates the radioactivity of [^{125}I]-5-iodouridine.

iodocytidine from C-U-A-C-C-A as either the 3′-phosphate or the dinucleotide Apio^{5}Cp, both of which elute with the solvent front on Aminex due to their negatively charged phosphate groups. By comparing the amount of adenosine to the radioactive iodine eluted at the front, one can use the Aminex analysis of the pancreatic RNase digest to readily calculate that there are 0.79 and 1.60 iodine atoms in each of the fragments 9b and 11b, respectively. It is well established that the Commerford procedure has an almost exclusive predilection to iodinate nonhelical residues (Batey & Brown, 1977); therefore C_{73} and C_{74} have been assigned as the two sites of iodination in the 3′-terminal fragment. The factors that reduced the apparent recovery of io^{5}C from the expected stoichiometries of 1.0 and 2.0 mol/mol of iodinated oligonucleotide must be operating equally in both fragments since the ratio of the observed stoichiometries is almost exactly 1:2.

Iodination of Uracil Occurs at U_8. Figure 5 shows that RNase T_1 should release U_8 in either of two fragments: the trinucleotide Upm^{1}Gpm^{2}Gp or the dinucleotide Upm^{1}G>P arising from partial RNase T_1 cleavage after m^{1}G. Holley and co-workers (Holley et al., 1965; Zamir et al., 1965) have shown that RNase T_1 cleaves slowly at m^{1}G to yield the cyclic 2′,3′-phosphate exclusively.

Figure 7 shows the Aminex profiles for the nucleoside composition of the oligonucleotides corresponding to the peaks 10a and 10b in the elution profile of the RNase T_1 digest shown in Figures 3a and 3b, respectively. Both fragments contained the modified nucleosides 1-methylguanosine and N^2-methylguanosine; this provides positive identification of the trinucleotide in each case. It is noteworthy that concomitant with the appearance of io^{5}U in this trinucleotide there was a substantial reduction in the amount of uridine, indicating that over half of the uridine in this fragment had been iodinated.

Peak 1b of the RNase T_1 elution profile (Figure 3b) contains the iodinated dinucleotide io^{5}Upm^{1}G>P. This was established in two experiments. First, the iodinated component of peak 1b was separated from overlapping fragments by chromatography on Vydac (Figure 8). The nucleoside content of the major radioactive fragment from Vydac was determined by digestion with the nuclease–phosphatase mixture (see Materials and Methods) and chromatography on Aminex (Figure 9). The analysis showed 200 pmol of 5-iodouridine (by radioactivity), roughly 50 pmol of adenosine (by absorbance), and possible traces of guanosine and cytidine. Clearly, 5-iodouridine was the only major nucleoside component; no 3′-terminal 1-methylguanosine was found nor expected since the cyclic 2′,3′-phosphate is resistant to bacterial alkaline phosphatase and would elute with the solvent front on Aminex A-6.

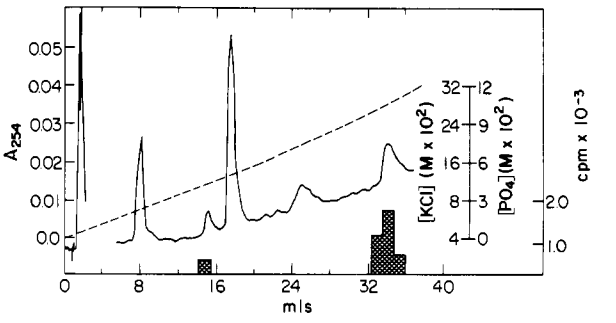

FIGURE 8: Separation of nucleotides in elution peak 1b of Figure 3b by further chromatography on Vydac. Appropriate fractions from Pellionex were collected on DEAE-cellulose, eluted, and lyophilized as described in the legend to Figure 4. The resulting powder was then dissolved in 100 μL of H_2O and applied to a 0.2 × 100 cm column of Vydac, jacketed and maintained at 50 °C. The concave elution gradient was formed by pumping 0.4 M KCl and 0.1 M KH_2PO_4, pH 2.9, into a mixing chamber which initially contained 50 mL of 0.001 M KH_2PO_4, pH 3.0. The column was pumped at ~80 psig for a flow rate of 12 mL/h.

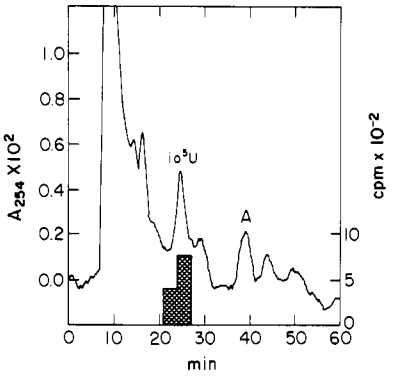

FIGURE 9: Nucleoside composition analysis of Aminex A-6 chromatography of the major radioactive elution peak from Vydac (Figure 8). Experimental details were the same as those given in Figure 4. The histogram indicates the radioactivity of [^{125}I]-5-iodouridine.

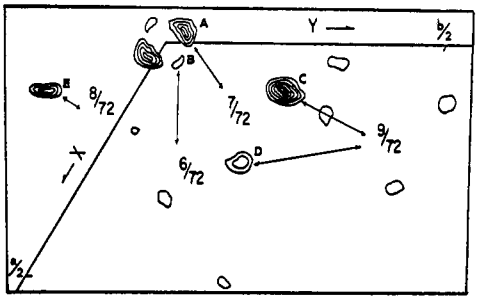

FIGURE 10: Three-dimensional difference electron-density map comparing the iodo derivative with the parent structure. A projection of four sections stacked perpendicular to c is shown, corresponding to an interval of $^4/_{72}$ along c. The contours are proportional to electron density, and all contours above zero are shown. The bold numbers give the fractional coordinates along c of the labeled peaks indicated by the double-headed arrows. c passes through the intersection of the axes. Due to the high symmetry of space group $P6_422$, this view includes all major features of the map. Relevant dyad axes are coincident with the x axis and the 6_4 screw axis through the origin.

In the second experiment, radioactive peak 1b was shown to be a partial digestion product of the iodinated trinucleotide io^{5}Upm^{1}Gpm^{2}Gp. This was done by isolating the trinucleotide io^{5}Upm^{1}Gpm^{2}Gp and subjecting it to further RNase T_1 digestion. The digest was combined with a RNase T_1 digest of native tRNA$_f^{Met}$ and cochromatographed on Pellionex (Figure 3d). Two peaks of radioactivity were seen in the elution profile; one was clearly the still intact trinucleotide, and the other

eluted exactly at the same position as the radioactive fragment in peak 1b.

Crystallographic Results. Figure 10 shows four superimposed sections of the three-dimensional difference Fourier synthesis projected down the crystallographic *c* axis. The peaks A, B, and C were assigned to specific iodinated residues on the basis of the following criteria: (a) integrated peak height from the difference map; (b) compatibility with chemical data, other marker studies, and our current map of yeast $tRNA_f^{Met}$.

Peak A, the second largest peak, is the easiest to assign. Its position, within the precision of a 6-Å map, coincides exactly with that found by Pasek et al. (1973) for iodine at io^5C_{73}, which was introduced by enzymatic degradation and resynthesis of the C-C-A terminus with nucleotidyl transferase and io^5CTP. Peak A disappears on a difference Fourier synthesis comparing our current iodo derivative with that of Pasek et al.; therefore, it is clearly due to iodine in io^5C_{73}.

Peak B is only slightly above noise level, but since (a) our chemical studies show two cytidines iodinated in the 3′-terminal hexanucleotide, (b) the reaction has a strong preference for single-strand cytidines, and (c) the peak-to-peak distance from A to B (6.7 Å) is within the expected limits for neighboring residues in a single-stranded region (Sussman & Kim, 1976), we have tentatively assigned peak B to iodine at io^5C_{74}.

Peak C is the largest peak on the difference synthesis; we have assigned it to the iodine atom of io^5U_8. Chemical analysis indicates that residue U_8 contains ~30% of the stably bound iodine and is the only major site of iodination outside the two sites in the 3′-terminal hexanucleotide; therefore, it is reasonable that is should give the largest peak on the difference map. Site C is sufficiently dense so that it is clearly seen on a two-dimensional projection difference Fourier synthesis of the iodo derivative vs. native $tRNA_f^{Met}$. Projection studies comparing thallium-soaked (see Materials and Methods) and native crystals show no peaks. This indicates that site C is due to iodine and not to thallium binding.

Peaks D and E were rejected as candidates for io^5C_{74} because they are too far (>25 Å) from the clearly established marker at C_{73}. As both D and E are less than half the occupancy of site C, they are less likely to be the highly reacted io^5U_8. Although sites D and E caused some initial uncertainty, it became clear that a consistent molecular interpretation of the electron density and other residue-specific markers presented itself if (and only if) the strongest peak (C) was assigned to the highly reacted io^5U_8. With appropriate caution we therefore proceeded on the presumption that peaks D and E did not represent one or more of the three stable covalently bonded iodine sites.

Discussion

The purpose of this study is to provide guidepoints for interpreting the electron density map of yeast $tRNA_f^{Met}$; to this end, we have iodinated residues U_8, C_{73}, and C_{74}. We have confirmed the position of the previously located C_{73} (peak A). Although the neighboring peak B was small, its position (6.5 Å from site A) strongly suggested that it was io^5C_{74}. The io^5U_8 marker, when assigned to peak C, suggested a particularly attractive interpretation for the course of the sugar–phosphate backbone within the 4.5-Å electron density map of yeast $tRNA_f^{Met}$, an interpretation which was also consistent with the markers at C_{73} and C_{74} and the osmium label on residue C_{38} (Rosa & Sigler, 1974). This interpretation (Figure 11) was subsequently verified by a successful crystallographic refinement to 4.0-Å resolution (Schevitz et al., 1979). There is no reason to suspect that the ability to isomorphously iodinate a limited number of residues in a crystalline tRNA is unique to this crystal structure. It might well be profitably applied to other crystallographic studies of tRNA.

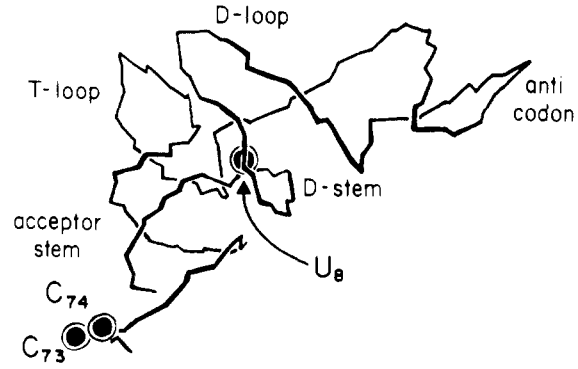

FIGURE 11: Positions of the three iodine markers at U_8, C_{73}, and C_{74} shown in relation to the *initial* interpretation of the course of the sugar–phosphate backbone. This rendering shows lines connecting alternating 3′ oxygens and phosphate moieties. Although suitable for illustrative purposes in the context of this paper, this illustration should not be taken as a definitive statement of the structure. The refined molecular model based on this initial interpretation confirms the iodine assignments (see text).

The crystallographic behavior of the marker atoms is in reasonable accord with our expectations regarding the relative flexibilities of different regions of the molecule. While our difference maps indicate almost twice as much iodine at U_8 as at C_{73} and show very little iodine at C_{74}, our chemical results suggest that all three sites are of comparable occupancy. An explanation of this discrepancy was suggested by the observations of Sussman & Kim (1976), who compared three refined models of yeast $tRNA^{Phe}$. They noted that the C-C-A terminus was the only region where significant discrepanices exist among these models and that in all cases the electron density in this region was weak. This has been recently borne out in the detailed refinement of the crystal structure of yeast $tRNA_f^{Met}$ and suggests that the single-stranded C-C-A end is, as expected from the lack of intramolecular constraints, a relatively flexible part of the tRNA molecule (Schevitz et al., 1979). Thus, in the absence of strong intermolecular constraints, the C-C-A terminus is likely to be a partially disordered region of the tRNA crystal structure. Disorder in the iodinated C-C-A terminus could easily account for the apparently low crystallographic occupancies of the iodine sites marking residues C_{73} and C_{74} and would explain the failure to achieve satisfactory refinement of Pasek's io^5C_{73} derivative (Pasek et al., 1973). The recently refined structure of yeast $tRNA_f^{Met}$ also suggests that the iodinated residues at the C-C-A terminus are displaced by 2–3 Å from their expected position in the native protein (A. Podjarny, R. Schevitz, J. Sussman, and P. B. Sigler, unpublished experiments). This local lack of isomorphism might further reduce the apparent iodine occupancy at these sites and confound the refinement of the heavy-atom parameters of the io^5C derivative of Pasek et al. (1973).

In contrast, residue U_8 of $tRNA_f^{Met}$ is likely to be subject to strong intramolecular constraints imposed by hydrogen-bonding and base-stacking interactions. This follows from the work of Robertus et al. (1974) and Kim et al. (1974), who have shown that in the crystal structure of yeast $tRNA^{Phe}$, U_8 pairs with A_{14} through a reverse Hoogsteen hydrogen-bonding scheme. Since U_8 and A_{14} are invariant residues [cf. Sigler (1975)], this base pair probably plays a central role in stabilizing the tertiary structure of all class I tRNAs (Levitt, 1969). To the extent that a similar arrangement obtains in all class I tRNAs, one would expect U_8 to be rigidly held in the crystal

structure of tRNA$_f^{Met}$. Recent analysis of the refined structure of yeast tRNA$_f^{Met}$ indicates that this is true. An iodine substituent at U_8 should therefore give a well-defined peak on a difference synthesis and would be expected to appear with higher occupancy than an iodine substituent at the C-C-A terminus. Indeed, the recent analysis of the refined structure (referenced above) shows the peak assigned to io$^5U_8$ to be located exactly at the 5 position of U_8.

The reactivity of U_8 deserves comment since previous work indicates that 5-iodocytidine is by far the major product of Commerford's iodination procedure and that iodination of single-stranded or, more correctly, nonhelical residues is strongly favored. Despite the probable involvement of U_8 in a tertiary hydrogen-bonded interaction, two observations suggest that its 5,6 double bond is accessible to attack by reagents in the solvent. First, the adjacent 4 position of residue s$^4U_8$ in *E. coli* tRNA$_f^{Met}$ has been shown to react with bulky photoaffinity and spin-labeling reagents (Schwartz & Ofengand, 1974; Daniel & Cohn, 1975). Second, a molecular model of the yeast tRNA^{Phe} structure as well as the current model of yeast tRNA$_f^{Met}$ shows that the 5,6 double bond of U_8 is much more exposed than that of a Watson–Crick base-paired pyrimidine in a helical region. Beyond the question of accessibility, we must assume that the local environment of U_8 in our crystal structure favors the formation of iodopyrimidine from the hydrated intermediate (Figure 1). This is in keeping with previous experience in which the unique local environments in a crystal may lead to unexpected reactions in the production of either coordinated or covalent heavy-atom derivatives (Sigler, 1970; Rosa & Sigler, 1974).

Acknowledgments

We thank Dr. Kan Agarwal for fruitful discussions concerning the identification of iodinated oligonucleotides, Richard Schevitz for the parent intensities, John Hughes and Richard Schevitz for advice and assistance with computations, and Joseph Rosa for advice on high-pressure chromatography. The SCAN11 densitometry software was generously provided by Dr. James Crawford of Harvard University; the γ-counting facilities were made available by the Chemistry Department of The Unversity of Chicago.

References

Adams, M. J., Hass, D. J., Jeffrey, B. A., McPherson, A., Mermall, H. L., Rossmann, M. G., Schevitz, R. W., & Wonacott, A. J. (1969) *J. Mol. Biol. 41*, 159.

Anderson, D. M., & Folk, W. R. (1976) *Biochemistry 15*, 1002.

Batey, I. L., & Brown, D. M. (1977) *Biochim. Biophys. Acta 474*, 378.

Commerford, S. L. (1971) *Biochemsitry 10*, 1993.

Daniel, W. E., & Cohn, M. (1975) *Proc. Natl. Acad. Sci. U.S.A. 72*, 2582.

Dunill, P., Green, D. W., & Simmons, R. M. (1966) *J. Mol. Biol. 22*, 135.

Holley, R. W., Everett, G. A., Madison, J. T., & Zamir, A. (1965) *J. Biol. Chem. 240*, 2122.

Johnson, C. D., Adolph, K., Rosa, J. J., Hall, M. D., & Sigler, P. B. (1970) *Nature (London) 226*, 1246

Kim, S.-H., Suddath, F. L., Quigley, G. J., McPherson, A., Sussman, J. L., Seeman, N., Wang, A. H. J., & Rich, A. (1974) *Science 185*, 435.

Levitt, M. (1969) *Nature (London) 224*, 759.

Marsh, D. J., & Petsko, G. A. (1973) *J. Appl. Crystallogr. 6*, 76.

Matthews, B. W., Cohen, G. H., Silverton, E. W., Braxton, H., & Davies, D. R. (1968) *J. Mol. Biol. 36*, 179.

Navia, M. A. (1974) Ph.D. Thesis, The University of Chicago.

Pasek, M., Venkatappa, M. P., & Sigler, P. B. (1973) *Biochemistry 12*, 4834.

RajBhandary, U. L., & Ghosh, H. P. (1969) *J. Biol. Chem. 244*, 1104.

Reeves, R. H., Imura, N., Schwam, H., Weiss, G. B., Schulman, L., & Chambers, R. W. (1968) *Proc. Natl. Acad. Sci. U.S.A. 60*, 1450.

Robertus, J. D., Ladner, J. E., Finch, J. T., Rhodes, D., Brown, R. S., Clark, B. F. C., & Klug, A. (1974) *Nature (London) 250*, 546.

Rosa, J. J., & Sigler, P. B. (1974) *Biochemistry 13*, 5102.

Schevitz, R. W., Krishnamachari, N., Hughes, J., Rosa, J., Pasek, M., Cornick, G., Navia, M., & Sigler, P. B. (1975) in *Structure and Conformation of Nucleic Acids and Protein–Nucleic Acid Interactions* (Sundaralingam, M., & Rao, S. T., Eds.) p 85, University Park Press, Baltimore, MD.

Schevitz, R. W., Podjarny, A. D., Krishnamachari, N., Hughes, J. J., & Sigler, P. B. (1979) *Nature (London) 278*, 188.

Schmidt, F. J., Omilianowski, D. R., & Bock, R. M. (1973) *Biochemistry 12*, 4980.

Schwartz, I., & Ofengand, J. (1974) *Proc. Natl. Acad. Sci. U.S.A. 71*, 3951.

Sigler, P. B. (1970) *Biochemistry 9*, 3609.

Sigler, P. B. (1975) *Annu. Rev. Biophys. Bioeng. 4*, 477.

Sigler, P. B., Jeffrey, B. A., Matthews, B. W., & Blow, D. M. (1966) *J. Mol. Biol. 15*, 175.

Sussman, J. L., & Kim, S.-H. (1976) *Science 192*, 853.

Tropp, J. (1976) Ph.D. Thesis, Department of Biochemistry, The University of Chicago.

Uziel, M., Koh, C. K., & Cohn, W. E. (1968) *Anal. Biochem. 25*, 77.

Wyckoff, H. W., Hardman, K. D., Allewell, N. M., Inagami, T., Tsernoglu, D., Johnson, L. N., & Richards, F. M. (1967) *J. Biol. Chem. 242*, 3749.

Zamir, A., Holley, R. W., & Marquisee, M. (1965) *J. Biol. Chem. 240*, 1267.